The role of novel iterative image reconstruction algorithms in coronary CT imaging

Doctoral Thesis

Bálint Szilveszter M.D.

Semmelweis University
Doctoral School of Basic Medicine

Supervisor: Pál Maurovich-Horvat, MD, Ph.D.
Official reviewers:
Tamás Györke, M.D., Ph.D. associate professor
Gergely Ágoston, M.D., Ph.D., assistant professor
Head of the Final Examination Committee:
Viktor Bérczi, MD, D.Sc.
Members of the Final Examination Committee:
Attila Doros, M.D., Ph.D.
László Sallai, M.D., Ph.D.

Budapest
2017

1. INTRODUCTION

In recent decades coronary computed tomography (CT) angiography (CTA) has emerged as a highly reliable and non-invasive modality for the detection of coronary artery disease (CAD). Prior landmark studies have extensively validated the diagnostic accuracy of coronary CTA versus the gold standard invasive coronary angiography (ICA). Current CT scanners with high temporal and spatial resolution are able to detect significantly more coronary lesions than ICA and are also able to depict adjacent cardiac and non-cardiac structures with great certainty. Importantly, coronary CTA is currently the only non-invasive imaging modality that can describe the extent, distribution and severity of non-obstructive CAD which has significant prognostic implications for patients with stable or acute chest pain.

Due to technological advancements, coronary CTA imaging allows for robust qualitative and quantitative assessment of atherosclerotic plaques. There are different methods to evaluate the extent and severity of CAD. Coronary artery calcium (CAC) scores measured by CT is a widely utilized, simple, reliable and useful tool for describing coronary plaque burden. Notably, recent studies suggest that CAC scoring has the ability to also re-stratify patient's risk and improve statin eligibility. Nonzero calcium score is associated with higher probability for obstructive CAD and increased risk for adverse cardiac events. CAC scores are measured using non-contrast CT images, however, subsequent contrast enhanced CTA of the coronaries also allows further differentiation of non-calcified or partially calcified plaques in the coronary system based on plaque composition.

The number of diagnostic cardiac tests has increased substantially in recent years and this has led to concerns attributable to increased radiation exposure. We have to ensure diagnostic image quality for all patients with lowest dose exposure reasonable achievable (as low as reasonably achievable – ALARA principle). There are several dose saving techniques and protocols that were introduced in daily practice to minimize CTA related dose exposure. CAC scoring was established on traditional Filtered Back Projection (FBP) images which are currently considered outdated as

novel reconstruction algorithms with robust image noise reduction became available. The increasing use of various iterative reconstruction (IR) techniques by all vendors holds the potential to significantly reduce radiation exposure and simultaneously improve image quality of coronary CT scans. Despite the widespread use, the influence of novel IR algorithms on coronary calcium scoring, plaque composition and subsequent individual risk assessment remains unclear. The current thesis aims to ascertain the role of novel IR algorithms on CT based plaque assessment and risk prediction.

1.1 Noninvasive coronary imaging using CT angiography

Coronary CT protocol typically consists of a non-enhanced prospectively ECG gated examination for calcium scoring followed by a subsequent contrast enhanced scan for the evaluation of the coronaries and cardiac structures. The non-enhanced scan ensures proper planning of the CTA including the length and position of the scan and the field of view. Non-contrast images are primarily used for calcium scoring. The scoring method was described by Agatston and is calculated from the calcified lesion area weighted by a density factor based on the voxel with the highest density. In a subsequent step with the administration of iodinated contrast material robust qualitative and quantitative characterization coronary plaques is feasible. On qualitative plaque assessment, we can distinguish between calcified, non-calcified or partially calcified plaques based on the extent of calcification in a given plaque. Also, current guidelines strongly encourage the assessment of high-risk plaque features such as positive remodeling, spotty calcium, napkin-ring sign (NRS) or low attenuation plaque.

1.2 Iterative reconstruction techniques in CT

Radiation exposure represents a major concern in coronary CTA due to potential risk of malignancy induction. The fragile balance between diagnostic image quality and applied radiation dose is an ongoing

challenge in CT imaging. Image quality is influenced by several factors including patient characteristics, scanner technology, imaging parameters and reconstruction algorithms. During the past few years a variety of iterative image reconstruction techniques have been introduced by all vendors in order to reduce radiation exposure of cardiac CT while maintaining or even improving image quality. Model based type of image reconstructions represents the latest advancement among image reconstruction techniques and thus limited data exists regarding the influence of this novel technique on plaque characterization and quantification. Despite recent advancements with robust noise reduction and advanced CT scanner technology, development of individualized dose saving strategies are necessary to meet the ALARA principle. In our study we evaluated the effects of a hybrid-type iterative reconstruction (HIR) and a model based iterative reconstruction (IMR) algorithm on calcium scoring, image quality and plaque assessment.

2. OBJECTIVES

2.1 Defining the impact of iterative reconstruction on calcium score and risk assessment

Despite the widespread use of novel reconstruction techniques, the model based IR techniques have not yet been validated for coronary calcification measurements in clinical setting. We sought to assess the impact of iterative model reconstruction on coronary artery calcium quantification as compared to the standard FBP algorithm and HIR. In addition, we aimed to simulate the impact of IR on CAC score based risk stratification of an asymptomatic patient population.

2.2 Defining the influence of iterative reconstruction on image quality

Excellent image quality is the prerequsite of accurate plaque assessment and thus patient management. Advancements in image reconstruction techniques hold the potential to provide better visualisation of coronary arteries by improving image quality. We aimed to further elucidate the impact of novel IR techniques (HIR and IMR) as compared to FBP on subjective and objective image quality for coronary artery analysis.

Comprehensive quantitative image quality analysis included signal- and contrast-to-noise calculations for proximal and distal coronary segments, whereas qualitative analysis aimed to evaluate the effects of IR on vessel sharpness and image noise on visual assessment.

2.3 Defining the changes in plaque quantification using iterative reconstruction

There is a growing body of evidence regarding the prognostic value of quantified coronary plaque volume for adverse events. We aimed to assess the impact of IMR on calcified plaque quantification as compared to FBP and HIR in coronary CTA. We hypothesize that novel model based IR could influence measured plaque volumes that ultimately influence individual risk assessment.

3. METHODS

3.1 Study design and study population for CAC based risk assessment

In a single center study, we performed CAC scoring in two distinct patient cohorts to evaluate the effects of novel IR methods. We enrolled 63 symptomatic patients referred to clinically indicated cardiac CT examination due to suspected coronary artery disease. On the basis of CAC score differences observed in the study population we subsequently simulated the effect of IR on the risk stratification in an asymptomatic test population of 504 individuals. First, we calculated the differences in total CAC score values between the different reconstruction methods. Second, relative differences were calculated by dividing the average difference of two reconstructions by the average of the minuend's total CAC score. Using the relative differences calculated on the study population, we multiplied the total CAC of the original FBP scores by the relative differences to get simulated HIR and IMR results on a patient basis. Subsequently we determined how many patients shifted from one risk group to another. Reclassification ratio was calculated by dividing the number of people who shifted from a given risk group by the total test population.

3.1.1 Coronary CT data acquisition and image analysis

All patients were scanned using a 256-slice CT-scanner (Brilliance iCT, Philips Healthcare, Best, The Netherlands). Oral beta-blockers were administered, if the heart rate exceeded 65 bpm.

We reconstructed axial images with 3 mm slice thickness using standard FBP, HIR (iDose4, Philips Healthcare, Cleveland, OH, USA) and IMR (Philips Healthcare, Cleveland, OH, USA) algorithms. We performed CAC scoring on the axial images using a commercially available software application (Heartbeat-CS, Philips Healthcare, Best, The Netherlands) according the Agatston-method. The software identified the coronary artery plaques with an area of $\geq 1 mm^2$ and a density of greater than 130 Hounsfield Units (HU). Subsequently coronary plaques were selected manually by the first observer which allowed the semiautomatic software to calculate CAC scores. The software also automatically calculates area and volume for coronary lesions. In addition datasets of 20 randomly selected patients were assessed two times by a second observer for calculating inter- and intra-observer variability. Patients were classified into the following risk categories based on the CAC score values: 0 normal/no risk, 1–10 low, 11–99 low-intermediate, 100–399 intermediate, 400 < high risk.

3.2 Study population for image quality and plaque analysis

We enrolled 52 consecutive individuals in a single center study who underwent routine clinical coronary CTA examination due to suspected CAD. Patients who had calcified and/or partially calcified plaque were included in the further analysis to study the effects of IR on plaque characteristics. To minimize the impact of motion artifact on image quality, patients with arrhythmia and/or with a heart rate of ≥65 beat per minute were also excluded.

3.2.1 Image quality assessment

We used a four point Likert-scale to analyze subjective image quality parameters on axial slices. Overall image quality was defined as a summary of image sharpness, image noise and blooming artifacts, if

present and categorized as follows: non-diagnostic (0); moderate, considerable artifacts with diagnostic image quality (1); good, minor artifacts (2) and excellent (3) image quality. Subjective noise was further analyzed and rated according to the graininess on the coronary CTA image: severe image noise (0); above average (1); average (2); no image noise (3).
On quantitative analysis, proximal and distal segments of the left anterior descending artery (LAD), circumflex artery (LCX) and right coronary artery (RCA) were evaluated. Circular regions of interest (3–4 mm^2) were manually placed in the coronary arteries and pericoronary fat to obtain median CT number in Hounsfield units. ROIs were placed in a homogenous region of the proximal and distal segments of LAD, CX and RCA and the correspondent areas of the pericoronary fat. Median image noise was determined as the standard deviation (SD) of the CT attenuation placed a circular ROI (200 mm^2) within the aortic root at the level of the LM coronary ostium. Signal-to-noise ratio (SNR) is defined as the CT attenuation value in a given segment divided by the image noise. Contrast to noise (CNR) ratios were calculated for all segments, as CNR = (HUlumen – HUfat) / image noise; HUlumen and HUfat represents the median CT attenuation in the coronary artery lumen and the pericoronary adipose tissue.

3.3 Semi-automated plaque assessment

We transferred the datasets present with any calcified or partially calcified plaque to a dedicated offline workstation (QAngio, version 2.1; Medis Medical Imaging Systems, Leiden, The Netherlands) for further plaque characterization. After automated segmentation of the coronary tree the proximal and distal end points of each plaque were set manually. Fully automated plaque quantification was performed without any manual corrections of boundaries to exclude the influence of observer bias. After automated delineation of the outer and inner vessel-wall boundaries we used the following fixed thresholds: calcified plaque volumes (>130 HU), non-calcified plaque volumes with high attenuation (90–129 HU), intermediate attenuation (30–89 HU) and low attenuation (<30 HU).

3.4 Statistical analyses

Continuous variables were presented as mean ± standard deviation or as medians with interquartile range (IQR) as appropriate depending on the distribution of the values, whereas categorical variables were expressed as percentage. The Kolmogorov-Smirnov test was applied to evaluate normality of continuous variables. The inter- and intra-reader agreement was calculated using Lin's concordance correlation coefficient. The following descriptive scale was used for values of the concordance correlation coefficient: <0.90 Poor, 0.90–0.95 Moderate, 0.95–0.99 Substantial, >0.99 Almost perfect. Our data was not normally distributed for CAC score, area and volume and therefore these parameters were compared by using the Friedman test using Bonferroni–Dunn test for post hoc multiple comparisons. Differences in risk stratification were also assessed using Chi-square test with Bonferroni correction.

The number of assessable segments for image quality analysis was compared using chi-square test. Plaque features and image quality parameters were not normally distributed and were compared by using the Friedman test with Bonferroni-Dunn test for post-hoc comparisons. The Wilcoxon signed rank test was used to assess the difference between image quality parameters of the proximal and distal vessel segments. The reproducibility of visual assessment of two observers was measured with kappa statistics interpreted as follows: $\kappa < 0.20$ poor, 0.21–0.40 fair, 0.41–0.60 moderate, 0.61–0.80 good, 0.81–1.00 very good. Statistical analysis was performed using SPSS (IBM Corp, version 22.0, Armonk, NY, USA). A p value of ≤ 0.05 was considered statistically significant.

4. RESULTS

4.1 Calcium score based risk reclassification by novel iterative reconstruction algorithms

In order to define the effects of IR on calcium score based risk predictions we analyzed a total of 63 patients and performed a simulation on the test population of 504 individuals. The median values of CAC scores were 147.7 (IQR 9.6–582.9), 107.0 (IQR 5.9–526.6) and 115.1 (IQR 9.3–508.3) for FBP, HIR and IMR, respectively. The minimum CAC score value was 0, whereas the maximum total CAC value was 2347.3 on FBP. The relative differences compared to FBP were −7.2 % for HIR and −7.3 % for IMR. Post-hoc analysis showed a significant difference in calcium scores between images reconstructed with HIR and IMR as compared to FBP ($p < 0.001$). However, calcium scores of images reconstructed with HIR and IMR did not differ ($p = 0.86$). Image noise decreased significantly with the use of IR: 40.1 ± 12.9 with FBP, 26.5 ± 7.2 with HIR and 13.7 ± 3.4 with IMR ($p < 0.001$). Calcium area values were 86.4, 74.6 and 67.0 mm^2, while calcium volume values were 129.9, 112.2 and 100.8 mm^3 for FBP, HIR and IMR, respectively. Both area and volume values were significantly lower with HIR and IMR as compared to FBP ($p < 0.001$), however there was no significant difference between HIR and IMR reconstructions ($p = 1.000$).

As compared to FBP, the utilization of HIR and iterative model reconstruction resulted in a modest reclassification rate among the low and intermediate groups of the study population; 6 of 63 patients were reclassified using HIR algorithm as compared to FBP. There was no significant difference between the three reconstruction techniques in risk categories ($p = 0.998$) **(Figure 1)**.

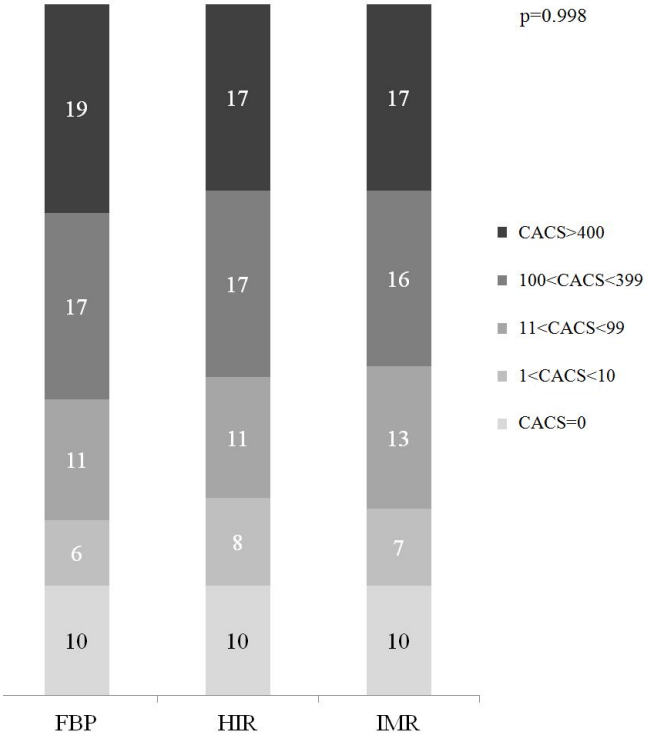

Figure 1. Coronary artery calcium score based risk categories of the study population.

The median CAC scores of the test population with FBP was 22.3 (IQR 0–199.2) (range of 0–4549.2). Based on our simulation the extrapolation of relative differences obtained by iterative algorithms yielded 2.4 % (12 patients) change in risk stratification in 504 individuals. Reclassification rate did not differ significantly among the 3 reconstructions (p = 0.998). All 12 patients were moved to lower risk groups based on their CAC values **(Figure 2)**.

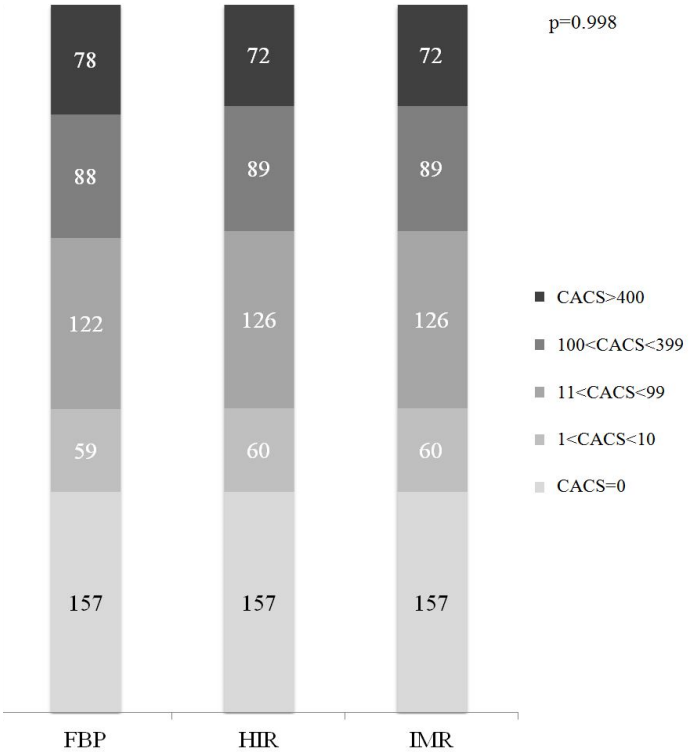

Figure 2. Risk reclassification based on CAC scores in the test population.

The inter-observer reproducibility of calcium scoring was substantial in images reconstructed with FBP (concordance correlation coefficient 0.973–0.986), whereas almost perfect reproducibility was found using IR techniques (HIR and IMR 0.990–0.997). Intra-observer correlation values were assessed in 20 patients with almost perfect concordance correlation coefficient values in all reconstructions (0.996–1).

4.2 Comparison of image quality parameters using different reconstructions

This study consisted of 52 patients with 468 triplets of coronary artery segments reconstructed with IMR, HIR and FBP. We identified 41 isolated calcified or partially calcified plaques.

Qualitative image analysis showed diagnostic image quality (rated as 1–3) in 453 segments (96.8%) with IMR, 437 (93.4%) with HIR and 407 (87.0%) with FBP ($p < 0.01$). Overall subjective image quality significantly improved with the application of HIR as compared to FBP, and further improved with IMR ($p < 0.01$ all) **(Figure 3)**. IMR yielded lower image noise by qualitative assessment as compared to HIR and FBP ($p < 0.01$ all). The majority of the coronary segments were rated as having no image noise (395/468, 84.4%), or average image noise (73/468, 15.6%) in the datasets reconstructed with IMR technique. The inter-reader reliability between the two readers was good for overall image quality (κ: 0.71), and image noise (κ: 0.73).

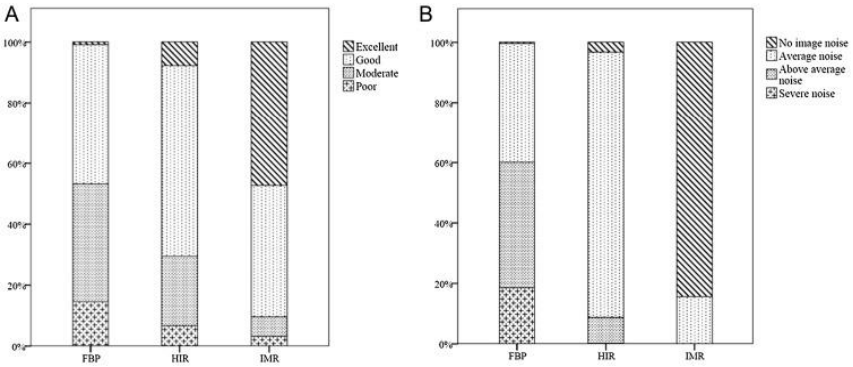

Figure 3. Visual assessment of image quality. A: Overall image quality, B: Image noise

On quantitative image quality analysis median HU in the aorta did not differ between the three reconstructions ($p = 1.00$). Higher luminal CT numbers ($p < 0.01$ all) were revealed in every assessed proximal and distal coronary artery segments with the use of IMR as compared to the other two reconstructions. No difference was observed between HIR and FBP for the respective coronary segment in HU values. Median attenuation values were similar or lower in the distal coronary segments using FBP and HIR reconstruction, as compared to the proximal coronary parts of the same vessel (LAD: $p = 0.71$ and $p = 0.69$; CX: $p < 0.01$ both, RCA: $p = 0.66$ and $p = 0.69$, respectively). Interestingly, IMR showed preserved or increased luminal contrast in the distal coronary segments as compared to the respective proximal coronary regions (LAD: $p < 0.01$; CX: $p = 0.18$; RCA: $p = 0.03$). Image noise in the aorta was significantly different for FBP, HIR and IMR (42.6 [33.2-48.3], 29.4 [23.0-33.1] and 12.4 [11.0-13.8], respectively, $p < 0.01$ all). Noise reduction achieved by HIR and IMR was 31.5% and 66.9% as compared to FBP, respectively. HIR improved CNR and SNR in all assessed coronary segments, as compared to FBP, which was further improved with IMR ($p < 0.01$, both). Inter-observer agreement between quantitative parameters was excellent with FBP, HIR and IMR reconstructions (correlation concordance coefficient: 0.97, 0.98 and 0.98, respectively).

4.3 Effects of iterative reconstruction on plaque assessment

Overall plaque volume was lower with HIR as compared to FBP ($p = 0.02$), and further reduced by IMR ($p < 0.01$ all). Calcified plaque volume was highest with FBP and lowest with IMR (FBP vs. HIR $p = 0.006$; HIR vs. IMR $p = 0.017$; and FBP vs. IMR $p < 0.001$). High attenuation non-calcified plaque volumes with an attenuation ranging 90–129 HU yielded similar values with FBP and HIR ($p = 0.81$), however it was lower with IMR (HIR vs. IMR $p = 0.002$ and FBP vs. IMR $p < 0.001$). No difference was found between FBP, HIR and IMR in intermediate and low attenuation non-calcified plaque components ($p = 0.22$ and 0.67, respectively). Lumen volumes did not differ between different reconstructions ($p = 0.23$). Overall plaque burden was lowest with IMR and highest with FBP (0.38 for IMR

[0.32–0.44], 0.42 for HIR [0.37–0.47] and 0.44 for FBP [0.38–0.50], $p < 0.05$ all). Volumes of various plaque components are summarized in Table 1.

Table 1. Plaque volume analysis with fixed threshold settings

Plaque volume values are presented in mm^3. Significant difference for all comparison combinations between the three reconstructions was assessed. Pairwise comparisons are represented between the three reconstructions as follows: *: $p<0.05$ FBP vs. IMR; †: $p<0.05$ HIR vs. IMR; ‡: $p<0.05$ FBP vs. HIR.

				Non-calcified plaque volume			Calcified plaque volume
	Vessel Volume *†	Lumen Volume	Overall Plaque Volume *†‡	<30 HU	30-89 HU	90-129 HU *†	>130 HU *†‡
FBP	334.1	186.0	147.0	1.5	8.2	10.2	115.9
HIR	327.6	186.6	138.7	1.4	7.7	9.7	110.2
IMR	308.0	190.9	121.7	1.1	6.0	7.2	105.9

5. CONCLUSIONS

In our study we found that IMR and HIR algorithms have led to substantial reduction in CAC scores. Changes in CAC score were associated with a modest reclassification rate in the study population. When translating the results to a larger test population, IR yielded a moderate reclassification rate of 2.4 % of 504 asymptomatic patients of a cardiovascular screening program. We did not detect the disappearance of calcium using IR algorithms. Also, we found excellent reproducibility of CAC using IR algorithms. The improved reproducibility of IR based CAC scoring could provide a more accurate risk prediction as compared to the noisier FBP images.

We demonstrated that the utilization of novel IR algorithms has led to significantly improved qualitative and quantitative coronary CTA image quality with improved visualization of the distal vessel segments as compared to traditional FBP. The number of non-diagnostic coronary segments were significantly lower using the most advanced model based IR technique as compared to traditional FBP. The use of novel IR algorithms is therefore strongly encouraged in clinical practice.

Furthermore, using automated plaque assessment we found that the use of IMR reduced both total and calcified plaque volume. Further studies are needed to evaluate the effects of these changes on individual risk prediction.

6. BIBLIOGRAPHY OF THE CANDIDATE'S PUBLICATIONS

6.1 Publications closely related to the present thesis

1. Szilveszter B, Elzomor H, Karolyi M, Kolossvary M, Raaijmakers R, Benke K, Celeng C, Bartykowszki A, Bagyura Z, Lux A, Merkely B, Maurovich-Horvat P. (2016) The effect of iterative model reconstruction on coronary artery calcium quantification. Int J Cardiovasc Imaging, 32: 153-160. IF:1.880

2. Karolyi M*, Szilveszter B*, Kolossvary M, Takx RA, Celeng C, Bartykowszki A, Jermendy AL, Panajotu A, Karady J, Raaijmakers R, Giepmans W, Merkely B and Maurovich-Horvat P. Iterative model reconstruction reduces calcified plaque volume in coronary CT angiography. Eur J Radiol. 2017;87:83-89. IF:2.593
3. Szilveszter B, Celeng C, Maurovich-Horvat P. (2016) Plaque assessment by coronary CT. Int J Cardiovasc Imaging, 32: 161-172. IF:1.880

6.2 Publications not related to the present thesis

1. Kolossváry M, Szilveszter B, Merkely B, Maurovich-Horvat P Plaque imaging with CT—a comprehensive review on coronary CT angiography based risk assessment. Cardiovascular Diagnosis and Therapy 10.21037/cdt.2016.11.06 IF:N/A

2. Meyersohn NM, Szilveszter B, Staziaki PV, Scholtz J-E, Takx RAP, Hoffmann U, Ghoshhajra BB, Coronary CT angiography in the emergency department utilizing second and third generation dual source CT. Journal of Cardiovascular Computed Tomograph (2017), doi: 10.1016/ j.jcct.2017.03.002. IF: 2,472

3. Janjua SA, Triant VA, Addison D, Szilveszter B, Regan S, Staziaki PV, Grinspoon SA, Hoffmann U, Zanni MV and Neilan TG. HIV Infection and Heart Failure Outcomes in Women. J Am Coll Cardiol. 2017;69:107-108. IF: 17.759

4. Farhad H, Staziaki PV, Addison D, Coelho-Filho OR, Shah RV, Mitchell RN, Szilveszter B, Abbasi SA, Kwong RY, Scherrer-Crosbie M, Hoffmann U, Jerosch-Herold M and Neilan TG. Characterization of the Changes in Cardiac Structure and Function in Mice Treated With Anthracyclines Using Serial Cardiac Magnetic Resonance Imaging. Circ Cardiovasc Imaging. 2016;9. IF: 5.744

5. Celeng C, Kolossvary M, Kovacs A, Molnar AA, Szilveszter B, Horvath T, Karolyi M, Jermendy AL, Tarnoki AD, Tarnoki DL, Karady J, Voros S, Jermendy G, Merkely B and Maurovich-Horvat P.

Aortic root dimensions are predominantly determined by genetic factors: a classical twin study. Eur Radiol. 2016. IF: 3.640

6. Edes IF, Ruzsa Z, Szabo G, Lux A, Geller L, Molnar L, Nowotta F, Hajas A, Szilveszter B, Becker D and Merkely B. Rotational atherectomy of undilatable coronary stents: stentablation, a clinical perspective and recommendation. EuroIntervention. 2016;12:e632-5. IF: 3.863

7. Kolossvary M, Szilveszter B, Edes IF, Nardai S, Voros V, Hartyanszky I, Merkely B, Voros S and Maurovich-Horvat P. Comparison of Quantity of Coronary Atherosclerotic Plaques Detected by Computed Tomography Versus Angiography. Am J Cardiol. 2016;117:1863-7. IF: 3.154

8. Benke K, Agg B, Szabo L, Szilveszter B, Odler B, Polos M, Cao C, Maurovich-Horvat P, Radovits T, Merkely B and Szabolcs Z. Bentall procedure: quarter century of clinical experiences of a single surgeon. J Cardiothorac Surg. 2016;11:19. IF: 1.036

9. Odler B, Cseh A, Constantin T, Fekete G, Losonczy G, Tamasi L, Benke K, Szilveszter B and Muller V. Long time enzyme replacement therapy stabilizes obstructive lung disease and alters peripheral immune cell subsets in Fabry patients. Clin Respir J. 2016. IF: 2.147

10. Maurovich-Horvat P, Tarnoki DL, Tarnoki AD, Horvath T, Jermendy AL, Kolossvary M, Szilveszter B, Voros V, Kovacs A, Molnar AA, Littvay L, Lamb HJ, Voros S, Jermendy G and Merkely B. Rationale, Design, and Methodological Aspects of the BUDAPEST-GLOBAL Study (Burden of Atherosclerotic Plaques Study in Twins-Genetic Loci and the Burden of Atherosclerotic Lesions). Clin Cardiol. 2015;38:699-707. IF: 2.431

11. Csobay-Novak C, Fontanini DM, Szilagyi BR, Szeberin Z, Szilveszter B, Maurovich-Horvat P, Huttl K and Sotonyi P. Thoracic aortic strain can affect endograft sizing in young patients. J Vasc Surg. 2015;62:1479-84. IF: 3.454

12. Benke K, Agg B, Matyas G, Szokolai V, Harsanyi G, Szilveszter B, Odler B, Polos M, Maurovich-Horvat P, Radovits T, Merkely B, Nagy ZB and Szabolcs Z. Gene polymorphisms as risk factors for predicting the cardiovascular manifestations in Marfan syndrome. Role of folic acid metabolism enzyme gene polymorphisms in Marfan syndrome. Thromb Haemost. 2015;114:748-56. IF: 5.255

13. Edes IF, Ruzsa Z, Szabo G, Nardai S, Becker D, Benke K, Szilveszter B and Merkely B. Clinical predictors of mortality following rotational atherectomy and stent implantation in high-risk patients: A single center experience. Catheter Cardiovasc Interv. 2015;86:634-41. IF: 2.181

14. Maurovich-Horvat P, Karolyi M, Horvath T, Szilveszter B, Bartykowszki A, Jermendy AL, Panajotu A, Celeng C, Suhai FI, Major GP, Csobay-Novak C, Huttl K and Merkely B. Esmolol is noninferior to metoprolol in achieving a target heart rate of 65 beats/min in patients referred to coronary CT angiography: a randomized controlled clinical trial. J Cardiovasc Comput Tomogr. 2015;9:139-45. IF: 2.472

15. Agg B, Benke K, Szilveszter B, Polos M, Daroczi L, Odler B, Nagy ZB, Tarr F, Merkely B and Szabolcs Z. Possible extracardiac predictors of aortic dissection in Marfan syndrome. BMC Cardiovasc Disord. 2014;14:47. IF: 1.916

16. Benke K, Agg B, Szilveszter B, Tarr F, Nagy ZB, Polos M, Daroczi L, Merkely B and Szabolcs Z. The role of transforming growth factor-beta in Marfan syndrome. Cardiol J. 2013;20:227-34. IF: 1.47

Articles in Hungarian

1. Benke K , Sayour AA , Ágg B , Radovits T , Szilveszter B , Odler B , Németh BT , Pólos M , Oláh A , Mátyás Cs , Ruppert M , Hartyánszky I , Maurovich-Horvat P , Merkely B , Szabolcs Z. (2016) Génpolimorfizmusok, mint rizikófaktorok a Marfan-szindróma kardiovaszkuláris manifesztációinak előrejelzésében Cardiologia Hungarica 46: pp. 76-81. IF:N/A

2. Bartykowszki A, Tóth L, Kerecsen G, Jermendy ÁL, Kolossváry M, Karády J, Szilveszter B, Károlyi M, Suhai F, Panajotu A, Kolozsvári R, Balázs Gy, Hüttl K, Thury A, Batthyány I, Kiss RG, Merkely B, Maurovich-Horvat P. (2017) A koronária-CT- angiográfia értelmezése és leletezése. A Magyar Kardiológusok Társasága Kardiovaszkuláris Képalkotó Munkacsoportjának ajánlása. Cardiologia Hungarica 47:(1) pp 2-9. IF:N/A
3. Benke K, Ágg B, Szilveszter B, Odler B, Nagy Zs, Pólos M, Merkely B, Szabolcs Z. (2014) A Marfan-szindróma molekuláris pathomechanizmusa. Cardiologia Hungarica 44(2):115-121. IF:N/A